

## Supplemental data:

### Structural Evidence for Enhancement of Sequential Vitamin D<sub>3</sub> Hydroxylation Activities by Directed Evolution of Cytochrome P450 Vitamin D<sub>3</sub> Hydroxylase

Yoshiaki Yasutake<sup>1</sup>, Yoshikazu Fujii<sup>2,3</sup>, Taiki Nishioka<sup>2</sup>, Woo-Kwang Cheon<sup>1</sup>, Akira Arisawa<sup>3</sup>, and Tomohiro Tamura<sup>1,2</sup>

From <sup>1</sup>Bioproduction Research Institute, National Institute of Advanced Industrial Science and Technology (AIST), Sapporo 062-8517, <sup>2</sup>Laboratory of Molecular Environmental Microbiology, Graduate School of Agriculture, Hokkaido University, Sapporo 060-8589, and <sup>3</sup>Bioresource Laboratories, Mercian Corporation, Shizuoka 438-0078, Japan.

## Supplemental table

**Table S1. Specific activities of Vdh-WT and Vdh-K1 against VD<sub>3</sub> and 25(OH)VD<sub>3</sub>.**

	Vdh-WT	Vdh-K1
VD <sub>3</sub> 25-hydroxylase activity (mmol/min/mol Vdh)	173.3 ± 10.7 (1.00)*	2,002 ± 361 (11.6)*
25(OH)VD <sub>3</sub> 1 $\alpha$ -hydroxylase activity (mmol/min/mol Vdh)	253.0 ± 4.5 (1.00)*	6,337 ± 383 (25.0)*

\*Relative activities are also given in parentheses.

## Supplemental figure legends

**Fig. S1. UV-visible absorption spectra for four single mutants (T70R (A), V156L (B), E126M (C), and E384R (D)) with  $\text{VD}_3/25(\text{OH})\text{VD}_3$ .** The absorption spectra were measured on addition of 0, 10 and 20  $\mu\text{M}$   $\text{VD}_3/25(\text{OH})\text{VD}_3$ , under the same buffer condition to Vdh-WT and Vdh-K1 shown in Fig. 2. Arrows indicate the directions of spectral changes in response to the increase in  $\text{VD}_3/25(\text{OH})\text{VD}_3$  concentrations. Wavelength (nm) at maximum height of Soret band observed in each spectral measurement is also indicated.

**Fig. S2. Difference distance (DD) matrix calculated by the program Superpose (1) for visualization of structural difference between Vdh-WT trigonal and orthorhombic forms (A) and between Vdh-WT trigonal form and Vdh-K1 (B).** DD matrix is a set of differences between the pairwise distance matrix of two molecules, where each distance matrix is generated by calculating the distances for all possible pairs of  $\text{C}\alpha$  atoms within a molecule. DD matrices are shown in white, 0–1.5; light green, 1.5–3.0; green, 3.0–5.0; dark green, 5.0–7.0; blue, 7.0–9.0; dark blue, 9.0–12.0; and black, over 12.0 Å. No conformational changes are observed between two crystal forms of Vdh-WT, whereas high DD values are calculated for residues ranges 150–190 and 205–220 between Vdh-WT and Vdh-K1. These regions roughly correspond to FG-helices and HI-loop, respectively.

**Fig. S3. Stereo view superposition of Vdh-WT (yellow), Vdh-K1 (blue), PikC open form (PDB code, 2BVJ; chain B; orange), and PikC closed form (PDB code, 2BVJ; chain A; green).** Heme cofactor from the Vdh-WT structure is in the sphere. The BC-loop, FG-loop, and HI-loop regions are indicated.

**Fig. S4. Simulated annealing 2Fo–Fc composite omit map for  $\text{VD}_3$  contoured at  $0.8\sigma$  and for  $25(\text{OH})\text{VD}_3$  at  $1.0\sigma$  in all five chains in the asymmetric unit.** The maps were generated by the program CNS 1.1 (2) using only protein models.

**Fig. S5. Comparison of active-site pocket of three VD<sub>3</sub> hydroxylating CYPs.** *A*, trigonal Vdh-WT bound with PEG (crystallization artifact). *B*, Vdh-K1 with bound VD<sub>3</sub>/25(OH)VD<sub>3</sub>. Both VD<sub>3</sub> and 25(OH)VD<sub>3</sub> are shown at substrate-binding site. *C*, CYP105A1 (P450 SU-1) R84A mutant from *Streptomyces griseolus* with bound the product 1 $\alpha$ ,25(OH)<sub>2</sub>VD<sub>3</sub> (PDB code, 2ZBZ). *D*, CYP2R1 with bound VD<sub>3</sub> (PDB code, 3C6G). Heme iron and the hydroxylating position of VD<sub>3</sub> (C1 or C25) are connected with dashed lines in orange.

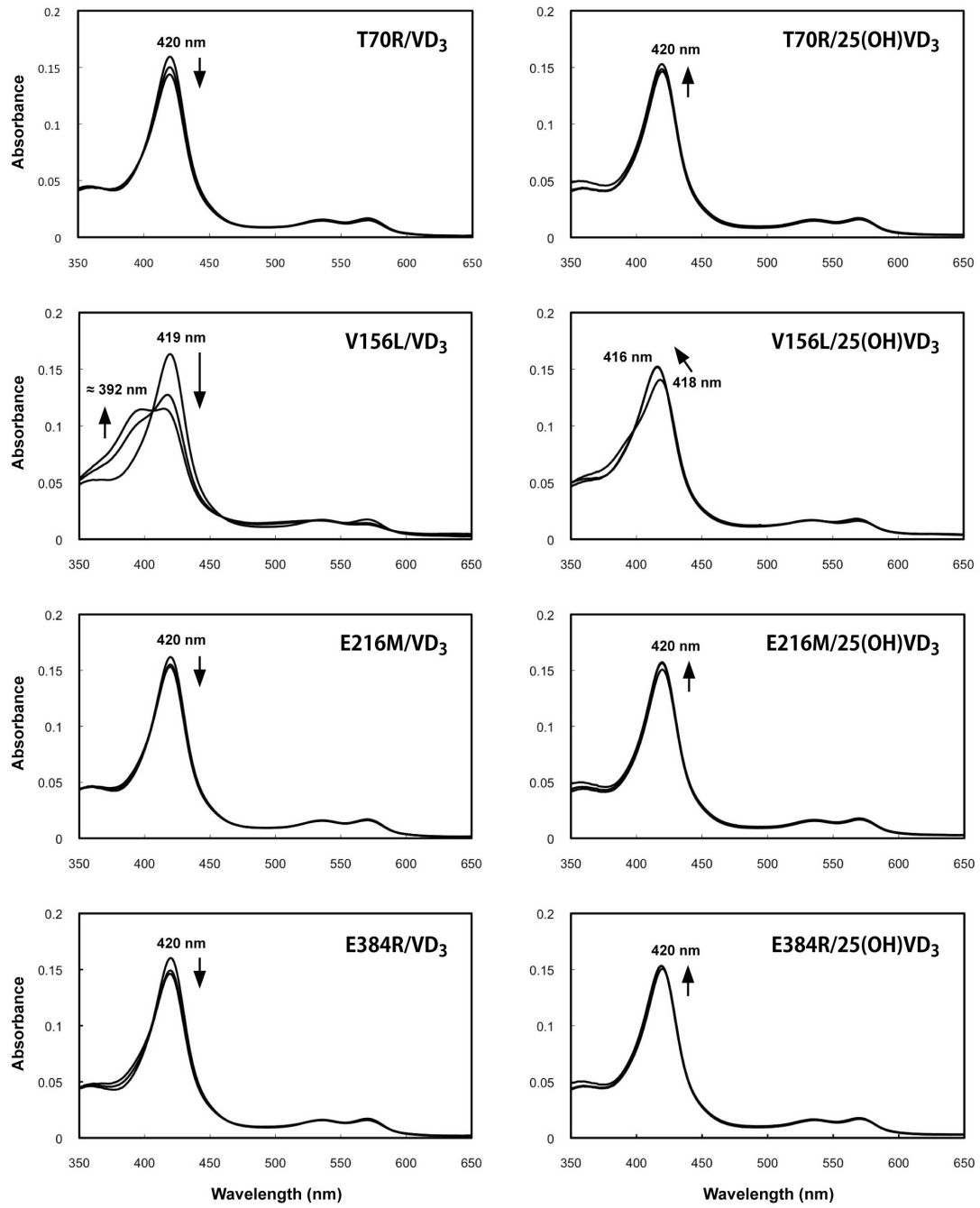
**Movie S1. Oscillation between Vdh-WT (open form) and Vdh-K1 with bound VD<sub>3</sub> (closed form).**

It should be noted that these two proteins forming open and closed states are not identical (four mutations were incorporated by directed evolution). The movie was created with the program PyMOL (3), using the atomic coordinates of Vdh-WT and Vdh-K1 and 15 additional atomic coordinate files, each consisting of 15 intermediate structures between Vdh-WT and Vdh-K1. The intermediate structures were generated by LSQMAN from the Uppsala Software Factory (4). The models include ribbon and line representation for all atoms except mutational residues. The models are colored according to the sequence using the rainbow color ramp going from N-terminus in blue to the C-terminus in red.

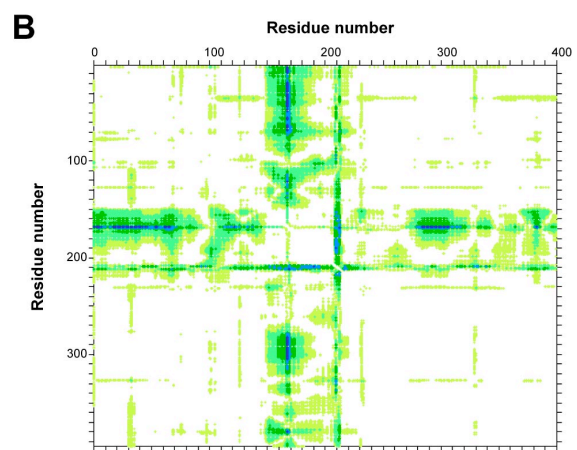
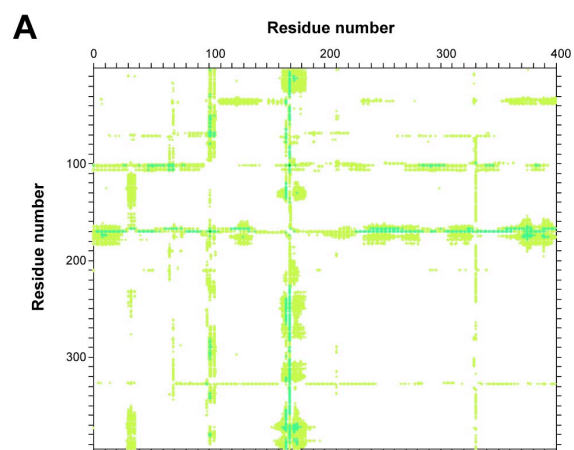
**Movie S2. The same as Movie S1 but from a different point of view.** The images in this movie were created by approximately 90° rotation of the images in Movie S1.

## Supplemental references

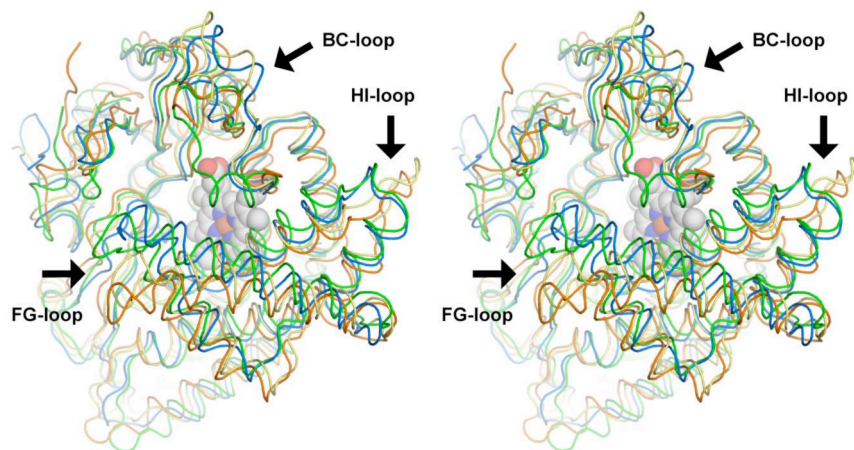
1. Maiti, R., Van Domselaar, G. H., Zhang, H., and Wishart, D. S. (2004) *Nucleic Acid Res.* **32**, W590–594
2. Brünger, A. T., Adams, P. D., Clore, G. M., DeLano, W. L., Gros, P., Grosse-Kunstleve, R. W., Jiang, J. S., Kuszewski, J., Nilges, M., Pannu, N. S., Read, R. J., Rice, L. M., Simonson, T., and Warren, G. L. (1998) *Acta crystallogr. Sect. D Biol. Crystallogr.* **54**, 905-921
3. DeLano, W. L. (2002) *The PyMOL Molecular Graphics System*, DeLano Scientific LLC, Palo Alto, CA
4. Kleywegt, G. J. (1999) *Acta Crystallogr. Sect. D Biol. Crystallogr.* **55**, 1878–1857



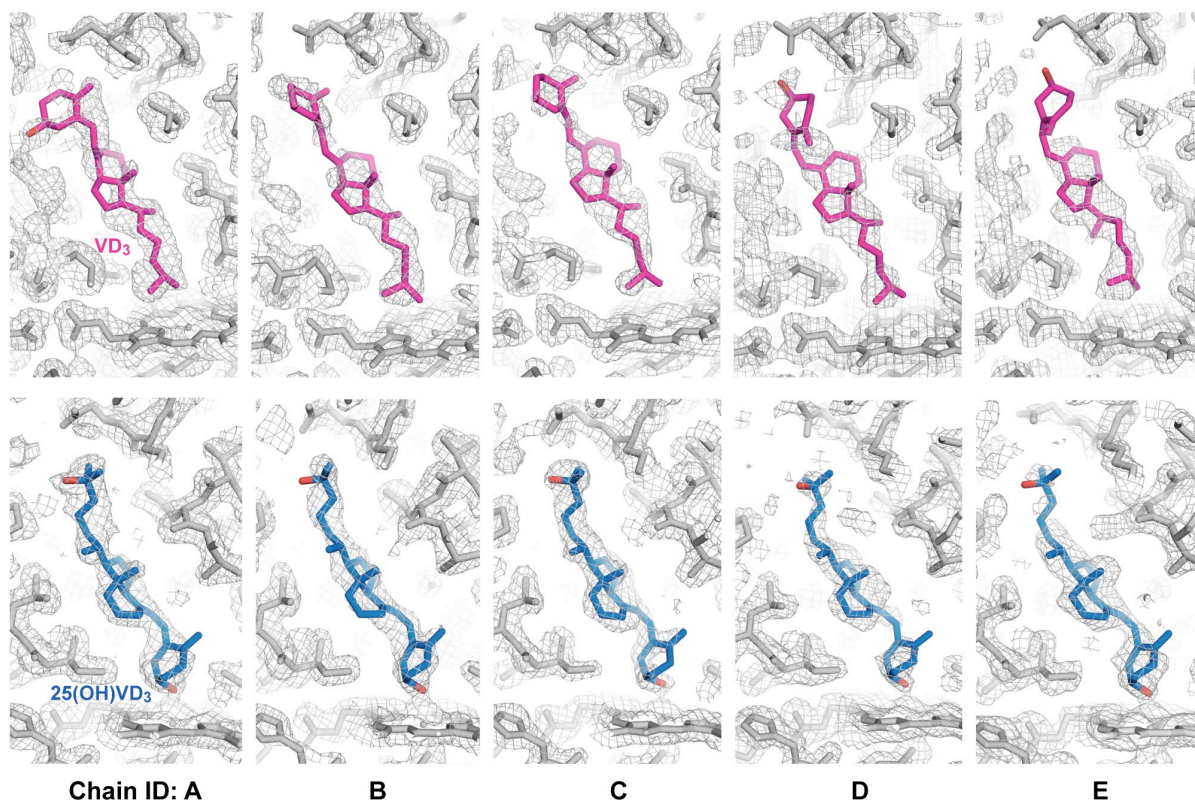
Supplemental Fig. S1



Supplemental Fig. S2

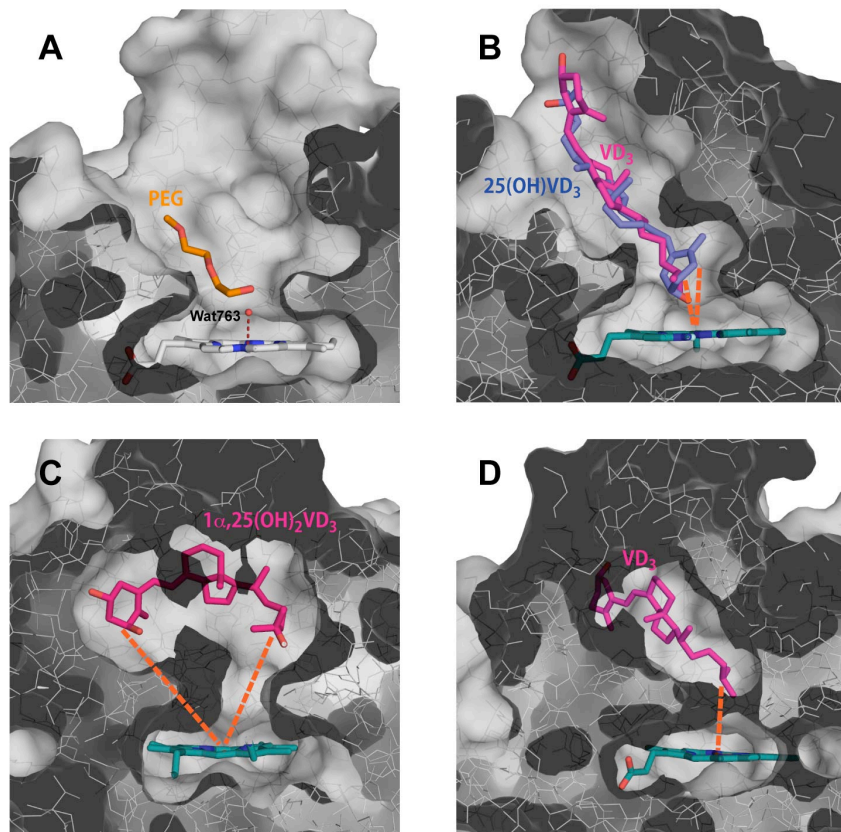


**Supplemental Fig. S3**



Supplemental Fig. S4





Supplemental Fig. S5